High Reliability Storage Systems for Genset Cranking

C. Boccaletti[1*], S. Elia[1], E. F. Salas M.[1], M. Pasquali[2]

[1] *Dept. of Astronautics, Electrical and Energetic Engineering, Sapienza University of Rome, Via Eudossiana 18, 00184 Rome, Italy;*
[2]*ENEA - Italian Agency for New Technologies, Energy and Sustainable Economic Development, Via Anguillarese, 301, 00123 Rome, Italy.*
** Corresponding author: chiara.boccaletti@uniroma1.it*

ABSTRACT - In many applications, like hospitals, the reliability of the emergency electrical supply is a critical issue, since the continuity has to be guaranteed at any time. The backup system usually consists of gensets and electrical starters (DC motors), supplied by lead-acid batteries. It is a fact that the latter are responsible for most genset cranking failures occurring in hospitals. Therefore, the reliability of the storage system should be improved to increase the Overall Mean Time Between Failures (MTBF) of the whole backup system. In this paper, eight different electrical storage systems have been modeled and simulated and they have been analyzed and compared from the point of view of reliability; in particular, the possibility of using supercapacitors (together with batteries or even replacing them) has been investigated. A huge number of real data regarding genset failures have been used, from both the literature and direct measurements made on purpose. An accurate statistical analysis has been performed to evaluate the MTBF for batteries, supercapacitors and other components available in the market, considering their actual characteristics. Finally, an innovative hybrid energy storage system has been proposed, based on both batteries and supercapacitors, allowing to triple the MTBF of the cranking storage system.

KEYWORDS - Mean Time Between Failures, Statistical data, Genset cranking, Starter motor, Electrical storage, Lead–Acid Batteries, Supercapacitors, Hospitals.

GLOSSARY

B	System with Batteries only
Bc	Battery charger
BS	Battery and Supercapacitor system
BSE	Battery and Supercapacitor system with Electronic control
BSR	Battery and Supercapacitor system with insertion Resistance
BI	Battery and Inductance system
BIS	Battery, Supercapacitor, and Inductance system
BISE	Battery, Supercapacitor, and Inductance system with Electronic control
BISR	Battery, Supercapacitor, and Inductance system with Insertion Resistance
BSSB	Battery Succor System between Batteries
EPR	Equivalent Parallel Resistance
ESR	Equivalent Series Resistance
MTBF	Mean Time Between Failures
PSE	Parallel Supercapacitors system with Electronic control
RBD	Reliability Block Diagram
SC	Supercapacitor
SE	Supercapacitor system with Electronic control
SOC	State of Charge
SOH	State of Health

1. INTRODUCTION

The continuity of supply is a critical issue in many applications, for which whatever break is not admissible, like for instance telecommunications, safety services, healthcare devices, etc. [1,2]. Gensets cranking has a fundamental role in hospitals, where a failure in the power supply represents a high-risk condition, implying not only economic losses, but also the possible loss of human lives [1]. Indeed, in absence of alternative power sources [3], the UPS of the operating rooms is available for no more than one hour. Thus, it is essential that the genset starts regularly. A huge number of statistical data have been collected during a period of ten years, from 300 gensets for healthcare applications [4]. It can be inferred that most of the unsuccessful gensets cranking are due to the failure of lead-acid batteries, quantified in at least 30% of total failures [5,6,7]. From the statistics, the percentage of non-functioning of the genset is equal to 7% of the interventions in a year. This percentage is subdivided into a 3% of failures in the batteries, a 3% failure in the re-fuelling system and a 1% relevant to the failure of the automatic transfer switch [8]. It should be noted that in hospitals the maintenance service regarding genset starting has a frequency of about one month. ENGIE (Italy) is a maintenance service company in charge of these interventions in hospitals, and thanks to its collaboration it was possible to obtain real data for this study from measurements on a 1000 kVA genset installed in a hospital in Rome (Italy). In addition, another important source of statistical data comes from the world of telecommunications. For instance, 100 gensets were tested by an Italian maintenance company

every six months for a duration of eight years, and also in this case there are 20% of cranking failures, out of which 80% is caused by degraded batteries (not yet published data). Even in large buildings that house vulnerable users, it is necessary to create a reliable emergency network to share and exchange energy in disaster conditions [9]. The network must be safe and reliable, in all conditions including blackout [10]. Through a suitable strategy, a correct energy flow inside a building can be ensured in any conditions, allowing the optimization of normal and emergency generation and storage systems [11]. The need to replace the lead batteries can be detected instrumentally when they are close to the non-operation limit, but it is necessary a system that still allows cranking even with a degraded storage system [12, 13]. In particular, it is necessary to have a high reliability of the systems also to guarantee the success of economic investments in hospitals [14].

In the following, eight different configurations of high-reliability alternative storage systems are investigated. Supercapacitors have a higher reliability and better technical performance than batteries, with particular reference to the inrush current which is much greater and does not change with time. Therefore, the possibility to combine batteries and supercapacitors has been also analyzed. In this work, an accurate study is carried out including the evaluation of the reliability of different systems for comparison. Although some tests on hybrid systems with batteries and supercapacitors can be found in the literature [15, 16], such an investigation, relying on real data from the specific application, represents a novel contribution. Actually, Section 2 is devoted to the analysis of the features of supercapacitors for genset cranking applications: typical ranges are given for each quantity. The mathematical models of the main components of a genset cranking system, to be integrated in the whole model used for the simulations, are described in Section 3. Section 4 is devoted to the model validation, by means of experimental data. In Section 5 the reliability parameters of each component are given. These parameters are then used to calculate the reliability of all the proposed storage systems. For each device configuration (Section 6) the Mean Time Between Failures (MTBF) is calculated by means of the Reliability Block Diagram (RBD) method [1]. For the sake of simplicity, RBD models are reported only for the main configurations. Finally, the conclusions are outlined in Section 7.

2. STATE OF THE ART OF SUPERCAPACITOR MANUFACTURING

More than 20 suitable supercapacitors by different manufacturers have been analyzed, taking into consideration the main electrical parameters and other characteristics. As a result, the average values are reported in Table 1. Figure 1 shows the exponential increase of the MTBF of supercapacitors with the reduction of the operating temperature [17]. The MTBF values are measured in years as given by the manufacturer, and the same unit is used in all the paper for the sake of comparison. On one hand, supercapacitors have a power density about 40 times greater than the power density of lead acid batteries; on the other hand, the energy density is about 8 times smaller than that of the batteries. Nevertheless, the stored energy is sufficient to satisfy the starting conditions of diesel generators. Therefore, the advantage of supercapacitors is the capability to quickly deliver a high power during the cranking phase, since no chemical conversion is involved like in batteries. Moreover, supercapacitors have a larger number of charge and discharge cycles (over 500,000), than batteries (lower than 1,000) [18]. As a result, closed systems for generator starting applications with supercapacitors only have been developed, known as GSS (Generator Starting System) [19]. The typical parameters of such systems are shown in Table 2.

Table 1: Average electrical parameters of supercapacitors per volume and weight.

Rated Voltage	Max. Voltage	Equivalent Series Resistance	Rated Capacity	Specific Capacity	Specific Energy	Specific Power	Price per liter and kilogram	Volume and Weight	Operating Temperature Range
2.7 [V]	2.85 [V]	0.289 [mΩ]	3000 [F]	7140 [F/L]	7.184 [Wh/L]	14.33 [kW/L]	122.3 [€/L]	0.44 [L]	[-40÷65] [°C]
				5485 [F/kg]	5.56 [Wh/kg]	11.08 [kW/kg]	94.6 [€/kg]	0.57 [kg]	

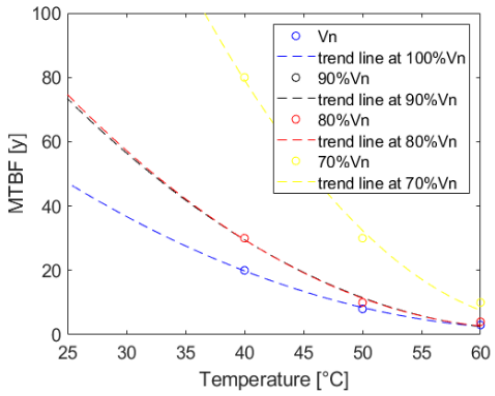

Figure 1: MTBF of supercapacitors vs. temperature for different voltage levels [17].

Table 2: Electrical parameters of GSS.

Capacity	Equivalent Series Resistance	Rated Voltage	Minimum Voltage	Maximun Voltage	Cold Cranking Amps	Storage Energy	Maximun Power	Weight
C [F]	ESR [mΩ]	Vn [V]	Vmin [V]	Vmax [V]	CCA [A]	E [Wh]	Pmax [kW]	W [Kg]
300-340	4	24	14.4	27	900 - 1100	30.4 - 38.4	45.6 - 50.8	7.8 - 8.2

3. MATHEMATICAL MODEL OF THE GENERATOR STARTING SYSTEM

The mathematical model of each element of the starting system, necessary for the simulations, has been developed as follows.

3.1 Battery model

The mathematical model of the batteries is based on the Shepherd's model [20]. The electrochemical processes taking place inside the battery are considered during both the charging and discharging phases. This model is defined by Equations 1 and 2.

$$\mathbf{V_{Batt}(t) = E_0 - K \cdot \frac{Q}{i_t - 0.1Q} \cdot (i(t) + i^*) - R \cdot i(t) + A \cdot e^{-B \cdot i_t}} \quad (1)$$

$$\mathbf{\dot{Exp}(t) = B \cdot |\, i(t) \,| \cdot [-Exp(t) + A \cdot u(t)]} \quad (2)$$

$V_{Batt}(t)$ is the voltage at the terminals [V], E_0 is the no-load voltage [V], K is the polarization constant or polarization resistance [V/Ah], Q is the capacity of the battery [Ah], i_t is its discharged capacity [Ah], A and B are parameters obtained from the battery datasheet: A is the amplitude of the exponential area [V], B is the inverse of the time constant of the exponential zone [Ah^{-1}]; R is the internal resistance of the battery [Ω]; i(t) is the dynamic battery current at time t [A], i^* represents the current filtered through polarization resistance [A], Exp(t) is the voltage in the exponential zone (discharge characteristic of the battery), u(t) indicates the charging mode (when equal to 1) or discharge mode (when equal to 0) of the battery [20]. The Matlab/Simulink model is represented in Figure 2. The main battery parameters used in the model are summarized in Table 3.

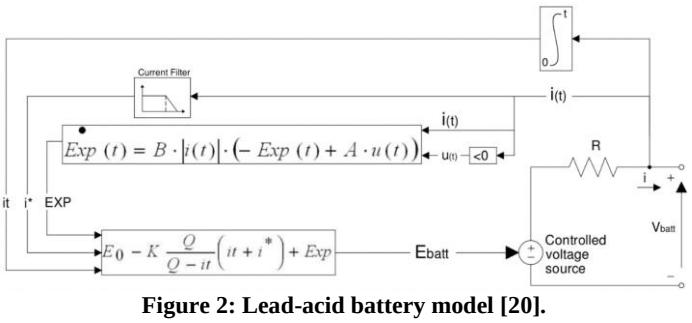

Figure 2: Lead-acid battery model [20].

Table 3: Characteristics of batteries for starting systems [21].

Electrical parameters				
Number of series batteries	Rated Voltage	Rated Capacity	Cold Cranking Amps	Internal resistance
Nº	Vn [V]	Cn [Ah]	CCA [A]	R [mΩ]
2	12	180	1150	4.17

3.2 Supercapacitor model

The equivalent circuit of the supercapacitors consists of a series connection of the equivalent series resistance (ESR) and the ideal capacity (C). The effect of the leakage current is represented by the equivalent parallel resistance (EPR) [22], considered only in open circuit conditions [18] (see Figure 3).
A more detailed mathematical model, capable of reproducing both the charging and discharging phenomena as a function of the materials and construction characteristics of the supercapacitor is described in [23, 24].

$$\mathbf{V_{SC}} = \frac{\mathbf{N_s Q_T d}}{\mathbf{N_p N_e \mathcal{E}\mathcal{E}_0 A_i}} + \frac{\mathbf{2N_e N_s RT}}{\mathbf{F}} \mathbf{sinh^{-1}}\left(\frac{\mathbf{Q_T}}{\mathbf{N_p N_e^2 A_i \sqrt{8RT\mathcal{E}\mathcal{E}_0 c}}}\right) - \mathbf{R_{SC}} \cdot \mathbf{i_{SC}} \quad (3)$$

V_{SC}, I_{SC} and R_{SC} are the voltage [V], current [A] and internal resistance [Ω] of the supercapacitor; N_e is the number of layers of the supercapacitor; N_s is the number of supercapacitors in series; N_p is the number of supercapacitors in parallel; $\mathcal{E}_0$ is the electrical permeability in the vacuum [F/m]; $\mathcal{E}$ is the dielectric permeability of the insulation; d is the distance between the electrodes [m]; A_i is the surface area between the electrodes and the electrolyte [m^2]; Q_T is the electric charge [C]; F is the Faraday's constant [C mol^{-1}]; R is the ideal gas constant [J/(mol K)]; T is the operating temperature [K]; c is the molar density [mol/m^3]. The Matlab/Simulink scheme is represented in Figure 4 and rated values used for the simulation are shown in Table 4.

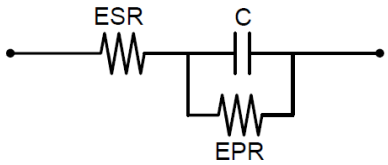

Figure 3: Equivalent circuit of the supercapacitor model [22].

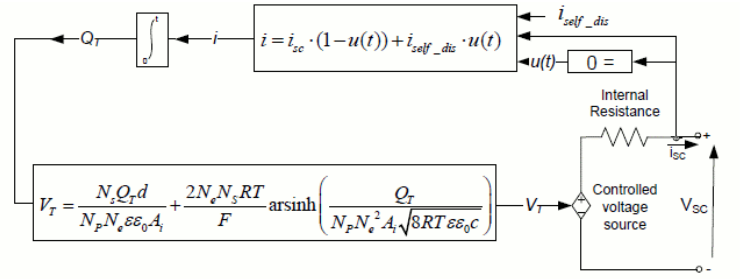

Figure 4: Scheme of the supercapacitor model [22, 23].

Table 4: Parameters of 9 Maxwell supercapacitor modules in series, model BCAP3000 [25].

Rated Capacity	Rated Voltage	Maximun Voltage	Maximun Current	Equivalent Series Resistance	Power	Energy	Specific Energy	Weight
C [F]	Vn [V]	Vmax [V]	Imax [A]	ESR [mΩ]	P [kW]	E [Wh]	ρE [Wh/kg]	w [kg]
333.33	24.3	25.7	1900	2.61	27.08	27.4	5.90	4.59

3.3 Starter motor model

The starter motor is a direct current machine with series excitation. The mathematical model is defined by electric equation 4 and dynamic equations 5 and 6.

$$\mathbf{V(t)} = \mathbf{R_e} \cdot \mathbf{i(t)} + \mathbf{L_e} \cdot \frac{\mathbf{di(t)}}{\mathbf{dt}} + \mathbf{R_a} \cdot \mathbf{i(t)} + \mathbf{L_a} \cdot \frac{\mathbf{di(t)}}{\mathbf{dt}} + \mathbf{e(t)} \quad (4)$$

$$\mathrm{j} \cdot \frac{\mathrm{d}\omega(\mathrm{t})}{\mathrm{dt}} = \mathrm{T_m(t)} - \mathrm{T_L(t)} - \mathrm{T_f(t)} \quad (5)$$

$$\mathrm{T_m(t)} = \mathrm{K_t} \cdot \mathrm{I(t)} \quad (6)$$

V(t) is the voltage at the machine terminals [V]; R_e and L_e are the resistance [Ω] and inductance [H] of the excitation circuit; R_a and L_a are the resistance [Ω] and inductance [H] of the armature circuit; e(t) is the back electromotive force; j is the moment of inertia of the motor [kg m^2]; ω(t) is the angular speed of the motor [rad/s]; $T_m(t)$ is the electromagnetic torque generated by the motor [Nm]; $T_L(t)$ is the load torque [N m]; $T_f(t)$ is the torque due to friction [N m]; I(t) is the current [A] and K_t is the torque constant of the machine [N m/A]. The simulations have been performed with the electrical parameters of a starter motor model Prestolite MS7-303P, reported in Table 5.

4. MODEL VALIDATION

The model of the starter motor has been validated by comparing the characteristic curves of the Prestolite MS7-303P starter motor with the simulations. The error is less than 3%.
To validate the whole starting system model, the current and voltage values obtained by simulation during the genset cranking phase have been compared with the ones experimentally measured by means of probes

and acquired through a digital oscilloscope PICOSCOPE 2406B, as shown in Figure 5 and Figure 6, respectively.
Based on the mathematical model of the starter motor and the measurements of voltage and current, it was possible to obtain the load torque by the diesel engine.

$$\mathbf{T_L(t) = -0.26\omega(t) + 69.17} \quad (7)$$

Table 5: Characteristics of Prestolite MS7-303P starter motor.

Prestolite MS7-303P: Starter motor (DC series excitation)							
Rated Voltage	Rated Power	Moment of Inertia	Time constant	Total Resistance	Total Inductance	Torque constant	BEMF constant
Vn [V]	Pn [kW]	J [kgm^2]	τ [ms]	Rm [mΩ]	Lm [μH]	Kt [Nm/A]	Ke [V/rpm]
24	9	0.0785	20	10	20	0.094	0.0094

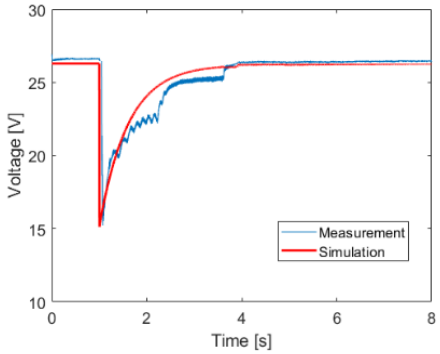

Figure 5: Measured (blue line) and simulated (red line) voltage at the battery terminals during start-up.

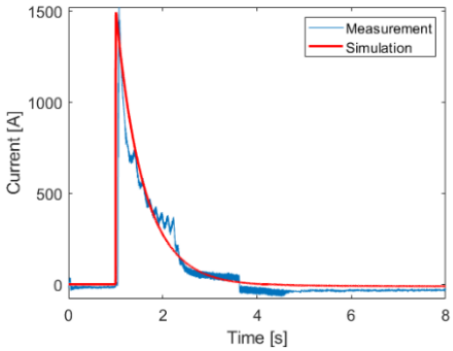

Figure 6: Measured (blue line) and simulated (red line) current drawn by the batteries during start-up.

5. SYSTEM RELIABILITY EVALUATION METHOD

The reliability of a system can be evaluated calculating the global MTBF through an RBD model [1]. The MTBF parameters of all the components are necessary for the evaluation of the global MTBF of each proposed system. They have been obtained performing an accurate statistical survey of literature and manufacturers' data. These reliability parameters are referred to a temperature of 40°C and are shown in Table 6. For the evaluation of the MTBF of a system composed by more than one component, the RBD method can be used. According to this method, the series connection of different components can be calculated by equation 8, and the parallel connection by equation 9.

$$\mathbf{MTBF_s = 1 \Big/ \sum_{i=1}^{n} \frac{1}{MTBF_i}} \quad (8)$$

$$\mathbf{MTBF_P = \int_0^{\infty} 1 - \prod_{i=1}^{N} \left(1 - e^{-\lambda_i t}\right) dt} \quad (9)$$

$MTBF_s$: is the equivalent MTBF of the components connected in series; $MTBF_i$ is the MTBF of i-th component, λ_i is the failure rate of i-th element; $MTBF_p$ is the equivalent MTBF of the components connected in parallel.

Table 6: Reliability parameters of each component of the proposed storage systems.

Component \ Parameter	Failure rate λ [F/y](1)	MTBF [y](2)	Reference
Battery	3.85E-01	2.6	[26]
Supercapacitor	0.05	20	[17]
Undervoltage relay	9.43E-03	106	[27]
Electromechanical contactor	1E-08	1E+08	[8]
Fuse	8.18E-02	12.22	[28]
Electronic control (El.Ctrl.)	1.33E-06	7.52E+05	[8]
Battery charger (Bc)	4.47E-03	223.71	[28]

(1) F = Failure; (2) y = years.

6. COMPARISON OF DIFFERENT CRANKING STORAGE SYSTEMS

6.1 System with batteries only (B)

Current genset cranking systems consist of a set of batteries that provide energy for the starter motor (see Figure 7). The speed curves of the starter motor vary according to the State Of Health (SOH) and State Of Charge (SOC) of the batteries. The minimum speed of the starter motor to meet the starting conditions is 1800 rpm [29]. Considering new batteries, a correct start occurs if the SOC is greater than 30%; for degraded batteries, the same condition is verified if the SOC is higher than 70%, as shown in Figures 8 and 9, respectively, where the dashed line indicates a failed cranking. The RBD of B system is that of Figure 10, from which it is possible to obtain: $MTBF_B = 1.3[y]$. The advantage of this system is the high rate of correct start-ups when the batteries are new. Defects in the system are due to the battery SOH. When batteries are degraded, a monthly maintenance program is needed to continuously check the SOC.

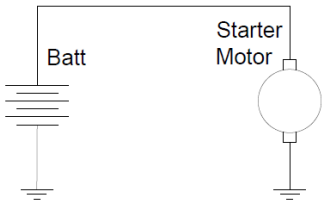

Figure 7: Scheme of a system with batteries only (B).

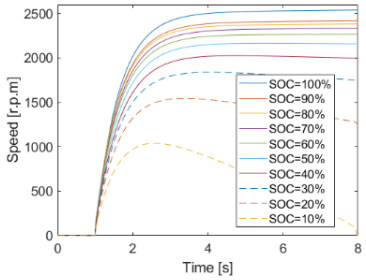

Figure 8: Speed of the starter motor as a function of the SOC considering new batteries.

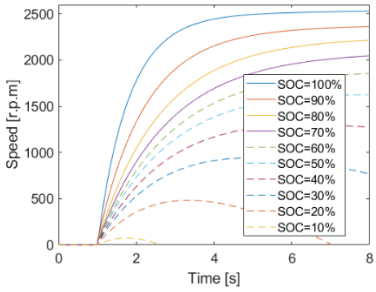

Figure 9: Speed of the starter motor as a function of the SOC considering degraded batteries.

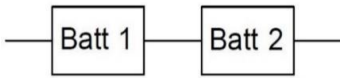

Figure 10: RBD of the batteries system (B).

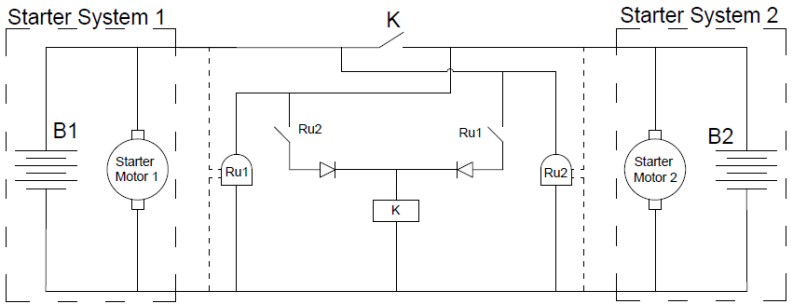

Figure 11: Scheme of the Batteries Succor System between Batteries (BSSB).

6.2 Battery Succor System between Batteries (BSSB)

The BSSB system (shown in Figure 11) provides a parallel connection between the battery systems of two adjacent groups B1 and B2. The connection is operated through the closure of electromechanical contactor K, which is controlled by the minimum voltage relay Ru, in case the state of the batteries of the main group cannot satisfy alone the minimum starting conditions. These two components must be appropriately sized and their reliability is fundamental for the correct functioning of the system. Simulations showed that the correct starting conditions are satisfied even in the case of degraded batteries, with SOC>30%. The RBD of BSSB system is shown in Figure 12; the system reliability is: $MTBF_{BSSB} = 1.94[y]$. Advantages of this system are: high percentage of correct start-ups even if the batteries are degraded; starting of the genset even with the main battery system completely degraded through the succor system; finally, in case of succor between the batteries it detects the degraded state of the storage system for possible extra-ordinary maintenance. These features allow BBSB system to be more reliable than the system with only one battery group. However, the drawback is the need of a starter system for each side.

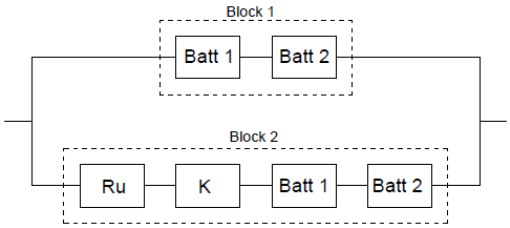

Figure 12: RBD of the Batteries Succour System between Batteries (BSSB).

6.3 Battery and Supercapacitor system (BS)

The storage system is realized through the parallel connection between batteries and supercapacitors as shown in Figure 13. Supercapacitors are protected by a fuse, which is set at the maximum current that the SCs can withstand for one second [25]. The supercapacitors are sized by considering the storage system voltage of 24 V, the maximum measured starting power equal to 23.3 kW and a third condition imposing the capability to supply enough energy for 5 consecutive startups, being the measured energy delivered in a cranking phase by the system with batteries equal to 4.55 Wh. The proposed storage system consists of the series connection of 9 single Maxwell BCAP3000 cells. The equivalent parameters are reported in Table **4**.

If the SCs are completely discharged, the inrush current would damage the entire storage system [30]. Thus, two systems are proposed: i. Charging through insertion resistance (BSR); and ii. Charging using electronic control (BSE). BSR system can be implemented through a pre-charging circuit with an insertion resistance equal to 300 mΩ, keeping the current below limits that do not cause degradation of the batteries. BSE system is implemented based on constant current and constant voltage (CCCV), but it is not recommended because of the sensitivity to noise, harmonics and failures due to overvoltage.

During the cranking phase, the starter motor speed reaches start-up conditions 4 times faster than the batteries only system. Moreover, as shown in Figure 14, the most significant inrush current is supplied by the SCs, while the maximum current provided by the batteries is reduced by 64% in comparison to the B system. The successful starting does not depend on the state of charge of the batteries. Neverthless, their role is crucial to ensure the full-charge state of SCs. The SC discharge after the event of a correct start, corresponds to a SOC decrease of 2.6%. If the batteries are completely discharged, a start-up is verified only if the SCs' SOC is higher than 95%, depending on their voltage drop [13]. Simulations results have shown that the self-discharge time leading to a SCs' SOC below 95% is equal to 1.6 days.

Block 1 in the schemes of Figures 15 and 16 includes a Batt*# value of MTBF that takes into account an enhanced value of reliability. Indeed, the presence of supercapacitors determines a lower battery stress and consequently a longer battery life [31, 32]. For the BSR system, MTBF is calculated through the RBD model shown in Figure 15: $MTBF_{BSR} = 3.91[y]$. For the BSE system, the RBD model is that shown in Figure 16, and $MTBF_{BSE} = 3.9[y]$. The advantages of this system are the following ones: the ability to guarantee start-up even in degraded battery conditions, since it is enough that the batteries keep the SC charged; the battery life is increased due to the lower stress during start-ups; BS system reaches the minimum conditions for starting more rapidly than the B system; BS system reliability can be considerably increased with the insertion resistance (BSR). The system drawback is the possible collapse of SC voltage if batteries are not available, compromising the starting process. Thus, a supervision every 1.6 days (38.4 hours) is necessary to verify the state of the storage system.

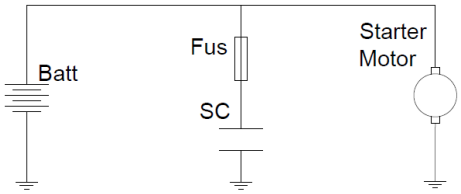

Figure 13: Scheme of the BS system.

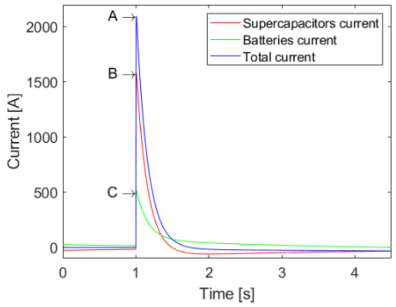

Figure 14: BS system currents at start-up. A: Max. total current (2100 A); B: Max. current supplied by SCs (1580 A); C: Max. current supplied by batteries (520 A).

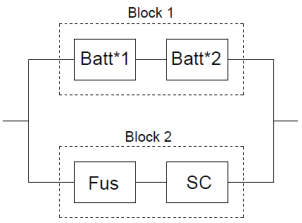

Figure 15: RBD of the battery and supercapacitor system with insertion resistance (BSR).

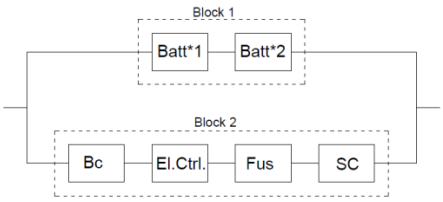

Figure 16: RBD of the Battery and Supercapacitor system with Electronic control (BSE).

6.4 Battery and Inductance System (BI)

If a limiting inductance is added with batteries only, from simulations MTBF value is 2.18 years. The limiting inductance lowers the battery stress during the cranking phase, thanks to the decrease of the peak inrush current value to some 300 A as shown in Figure 17, in this way increasing the battery life duration. If appropriately sized, the inductance does not affect start-ups in comparison with B system. For the simulations, an iron inductance $L = 1[mH]$ has been considered, with a resistance $R_L = 3.6[m\Omega]$ [33].

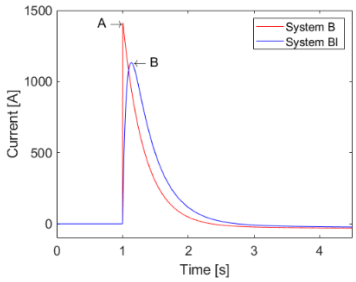

Figure 17: Comparison of the starting current of B and BI systems considering new and fully charged batteries. A: Max. current reached by B system; B: Maximum current reached by BI system.

6.5 Battery, Supercapacitor, and Inductance System (BIS)

The BIS system has the same scheme as the BS system of Figure 13, but with the insertion of a limiting inductance between the storage components. During the cranking phase, the current supplied by the batteries is reduced by about 50% in comparison with the BS system, reaching a maximum value of 280 A.
The analysis of the reliability has been made considering two possible solutions for the charging phases: i. BIS with insertion resistance (BISR), $MTBF_{BISR} = 4.11[y]$ (see Figure 18); ii. BIS with electronic control (BISE), $MTBF_{BISE} = 4.1[y]$ (see Figure 19). The inductance limits the current supplied by the battery taking advantage from the SC; therefore, the reliability of this system increases even more with respect to BS system.

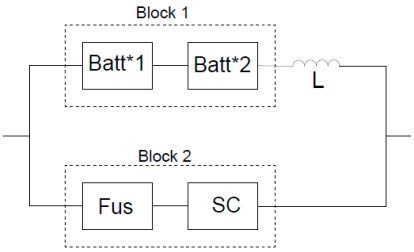

Figure 18: RBD diagram of the BISR system.

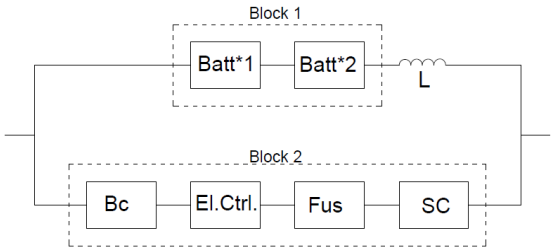

Figure 19: RBD diagram of the BISE system.

6.6 Supercapacitor System (SE)

Storage systems with supercapacitors only (SE) must be charged by an electronic control as shown in Figure 20. The corresponding RBD diagram is depicted in Figure 21. The system can ensure up to two successful startups only if SOC>95%. To ensure the start-up even for a lower SOC, a second group of supercapacitors is connected in parallel to the first one, with the same characteristics and fuse protection (PSE system). Both branches are charged by the same electronic control (Figure 22). In this case, a SOC>90% is enough to guarantee twice more events than the simple SE system. The high SOC values required for a correct start are due to the collapse of the SC voltage after the startup phase [13].
The analysis of the reliability is made considering a single or double branch of SCs, through the block diagrams shown in Figures 21 and 22, respectively. The results of the RBD analysis are the following. SE:

$MTBF_{SE} = 1.86[y]$; PSE: $MTBF_{PSE} = 2.8[y]$. The advantage of SE system is the increase in reliability compared to the system with only batteries. However, it is necessary a high value of SCs' SOC to guarantee a successful startup. In case of failure, the start-up is compromised in a very short time due to SC leakage currents; moreover, electronic controls are not reliable in abnormal conditions of the powering circuits.

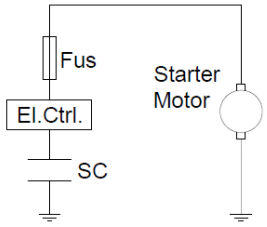

Figure 20: Scheme of the SC system with Electronic Control (SE).

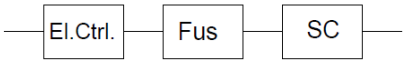

Figure 21: RBD diagram of the SC system with electronic control (SE).

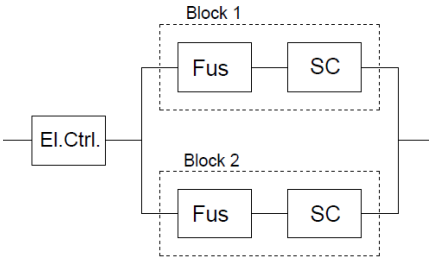

Figure 22: RBD diagram for the system with two equal branches of SCs with electronic control (PSE).

6.7 Discussion.

A comparison of the above systems through the MTBF parameter is shown in increasing order in Figure 23. For each system, the initial cost for implementation is shown in per unit [p.u.], based on the cost of the current battery system. From Figure 24, it is then evident that the reliability of systems with supercapacitors increases when the operating temperature decreases. For storage systems including supercapacitors it is strongly recommended to install them in rooms with temperatures below 25°C or adequately cooled.

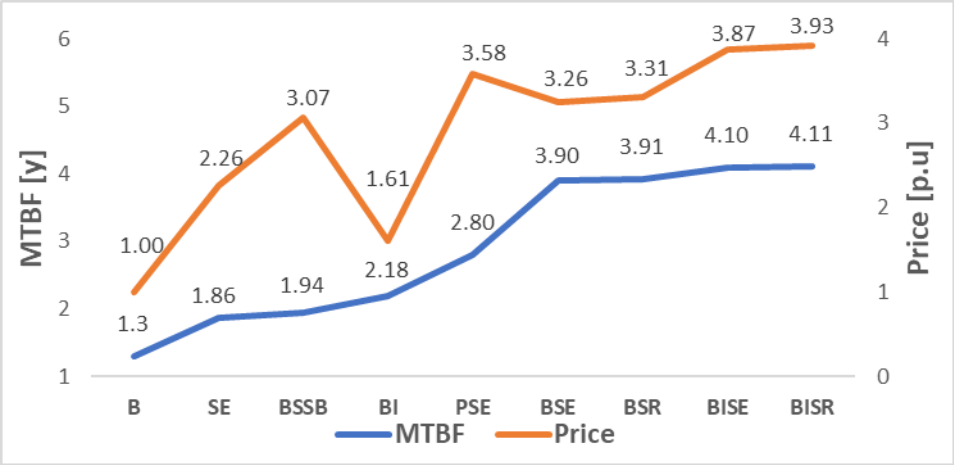

Figure 23: MTBF and initial costs of each proposal.

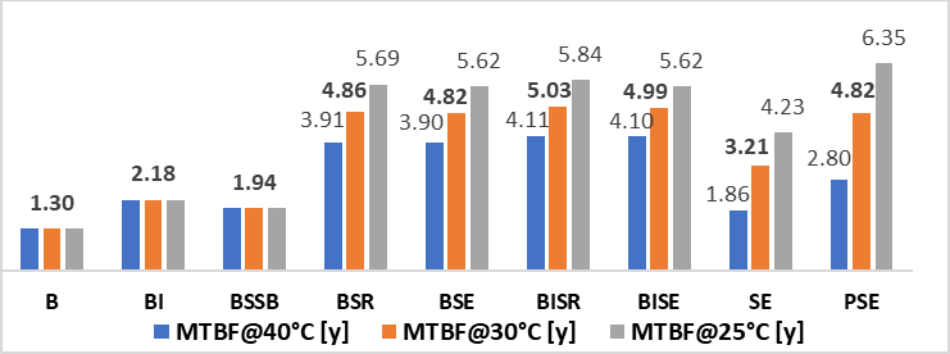

Figure 24: MTBF as a function of temperature, for all the proposed systems.

7. CONCLUSIONS

Nowadays the energy storage for emergency genset cranking is provided only by lead-acid batteries: a fail of these accumulators could easily lead a hospital to a blackout. Since such occurrence implies high risks for

human life, the possibility to effectively increase the reliability of genset cranking systems without adopting complex and/or expensive configurations is an important issue.
This work has demonstrated that the use of supercapacitors in starting systems strongly improves the reliability of gensets. Eight different innovative solutions to improve the reliability of traditional storage systems have been proposed and evaluated. The best solution proposed here (BISR), with an MTBF of 4.1 years, takes into account a simple series insertion of a limiting inductance in the battery output and of a supercapacitor in parallel. With the proposed solution, the MTBF of the cranking storage system is increased by three times compared to the standard systems based on batteries only. The cost of such systems are absolutely reasonable, being about four times that of traditional systems based on batteries. All configurations analyzed here can be easily assembled using components available on the market. Moreover, all the proposed systems are characterized by a simple electrical scheme and easy management and maintenance. In particular, the proposed solution is based on low-complexity technologies, implicitly more reliable and with reduced maintenance needs, differently from other solutions mainly based on additional electronic components [6].
With the best identified solution (BISR), the risk of cranking failure is strongly reduced with respect to the B system, ensuring starting even in degraded battery conditions up to a residual SOC of 10%. Moreover, the life of the batteries is extended, avoiding their frequent inspection and replacement [7]. The proposed scheme is suitable to many other important stand-alone applications such as civil construction sites, safety systems, etc., and can contribute to manage peak demands in any high power device [34]. With the proposed system, the storage MTBF is about 50 months, while the frequency of the maintenance start-up test of the genset is one month: for this reason, it is certainly possible to identify the state of degraded batteries well in advance, preventing from any problem [12]. Finally, the above discussion suggests the need for a new technical standard on the subject: all genset manufacturers should be compelled to install an additional succor storage or provide a more reliable one.

ACKNOWLEDGEMENTS

Data collection was performed with the support of ENGIE maintenance supervisor Mr. Mario Longo.
This research did not receive any specific grant from funding agencies in the public, commercial, or not-for-profit sectors.

REFERENCES

[1] S. Elia, A. Santantonio, Fire Risk in MTBF Evaluation for UPS System, Advances in Electrical and Electronic Engineering, 14(2), 2016, pp. 189–195, DOI:10.15598/aeee.v14i2.1662.
[2] E. F. F. Ribeiro, A. J. M. Cardoso, C. Boccaletti, Reliability Issues of Renewable Energy Based Power Systems for Telecommunications, in: Manuel Pérez-Donsión, Silvano Vergura, Gianpaolo Vitale Eds., Renewable Energy/Selected Issues, Volume I and II, 1237, ISBN-10: 1443888036, ISBN-13: 978-1443888035, Cambridge Scholars Publishing; 1st edition, 2016.
[3] F. Muzi, L. Calcara, S. Sangiovanni, M. Pompili, Smart Energy Management of a Prosumer for a Better Environment Safeguard, 110th AEIT International Annual Conference, Bari, Italy, 2018, DOI:10.23919/AEIT.2018.8577434.
[4] R. M. Visconti, D. Morea, Big Data for the Sustainability of Healthcare Project Financing, Sustainability, 11(13), 3748, 2019, DOI: 10.3390/su11133748.
[5] Y. Du, J. Burnett, S.M. Chan, Reliability of Standby Generators in Hong Kong Buildings, IEEE Transactions on Industry Applications, 39(6), 2003, DOI:10.1109/TIA.2003.818978.
[6] Wickramasinghe, W.M.H.R., Duleeka, K.T.G.M., Kolamunna, H.D., Abeyratne, S.G., A power electronics assisted emergency vehicle starter, 16th International Power Electronics and Motion Control Conference and Exposition, 21-24 Sept. 2014, DOI: 10.1109/EPEPEMC.2014.6980506.
[7] Mürken, M., Kübel, D., Thanheiser, A., Gratzfeld, P., Analysis of automotive lead-acid batteries exchange rate on the base of field data acquisition, IEEE International Conference on Electrical Systems for Aircraft, Railway, Ship Propulsion and Road Vehicles & International Transportation Electrification Conference (ESARS-ITEC), 7-9 Nov. 2018, DOI: 10.1109/ESARS-ITEC.2018.8607507.
[8] S. Elia, E. Santini, M. Tobia, Comparison between Different Electrical Configurations of Emergency Diesel Generators for Redundancy and Reliability Improving, Periodica Polytechnica Electrical Engineering and Computer Science, 62(4), 144-148, 2018, DOI:10.3311/PPee.13242.
[9] R. Lamedica, F. Muzi, A. Prudenzi, S. Elia, L. Podestà, A. Ruvio, S. Sangiovanni, E. Santini, F. Trentini, Electrical and thermal integrated load management of tertiary buildings, International Review of Electrical Engineering, 13(4), 276-289, 2018, DOI: 10.15866/iree.v13i4.15193.
[10] A. Pieroni, N. Scarpato, L. Di Nunzio, F. Fallucchi, M. Raso, Smarter City: Smart energy grid based on Blockchain technology, Int. J. on Advanced Science, Engineering and Information Technology, 8 (1), 298-306, 2018, DOI: 10.18517/ijaseit.8.1.4954
[11] F. Muzi, L. Calcara, M. Pompili, S. Sangiovanni, The New Prosumer Tasks in the Energy Management of Buildings, 2018 IEEE Int. Conf. on Environment and Electrical Engineering and 2018 IEEE Industrial and Commercial Power Systems Europe, Palermo, Italy, 2018, DOI: 10.1109/EEEIC.2018.8494537.

[12] Salloux, K., McHardy, J., Eliminating battery failure - two new leading indicators of battery health - a case study, INTELEC 07, 29th International Telecommunications Energy Conference, 30 Sept.-4 Oct. 2007, DOI: 10.1109/INTLEC.2007.4448765.
[13] Kroics, K, System for start of internal combustion engine with hybrid battery-supercapacitor source, 56th Int. Scientific Conf. on Power and Electrical Engineering of Riga Technical University (RTUCON), 2015, DOI: 10.1109/RTUCON.2015.7343167.
[14] R. M. Visconti, L. Martiniello, D. Morea, E. Gebennini, Can public-private partnerships foster investment sustainability in smart hospitals?, Sustainability, 11(6), 1704, 2019, DOI: 10.3390/su11061704.
[15] Liu, H., Wang, Z., Cheng, J., Maly, D., Improvement on the Cold Cranking Capacity of Commercial Vehicle by Using Supercapacitor and Lead-Acid Battery Hybrid, IEEE Transactions on Vehicular Technology (Volume: 58 , Issue: 3 , March 2009), DOI: 10.1109/TVT.2008.929220.
[16] Yadav,V.K., Bhardwaj, N., "Introduction to Supercapacitors and Supercapacitor Assisted Engine Starting System" International Journal of Scientific & Engineering Research, Volume 4, Issue 8, August-2013 583, ISSN 2229-5518.
[17] AVX, SCC series, High Capacitance Cylindrical SuperCapacitors datasheet, licensed by CAP-XX, 2019.
[18] V. A. Shah, P. Kundu, R. Maheshwari, Improved Method for Characterization of Ultracapacitor by Constant Current Charging, Int. J. of Modeling and Optimization, 2(3), 2012, DOI: 10.7763/IJMO.2012.V2.129.
[19] Maxwell Technologies Enabling Energy's Future, Generator starting solutions: 2-3 Terminal Series, GSS datasheet, 2016.
[20] O. Tremblay, L.-A. Dessaint, Experimental validation of battery dynamic model for EV application, World Electric Vehicle Journal, 3(2), 289-298, 2009, DOI:10.3390/wevj3020289.
[21] Trojan Battery Company, Reliant Battery, 31-AGM datasheet, 2018.
[22] W. Kai, R. Baosen, L. Liwei, L. Yuhao, Z. Hongwei, S. Zongqiang, A review of Modeling Research on Supercapacitor, State Grid Shandong Electric Power Maintenance Company, 250021 Jinan, China, DOI: 10.1109/CAC.2017.8243857.
[23] N. Xu, J. Riley, Nonlinear analysis of a classical system: The double layer capacitor, Electrochemistry Communications, 13, 1077–1081, 2011.
[24] K. Oldham, A Gouy Chapman–Stern model of the double layer at a (metal)/(ionic liquid) interface, J. of Electroanalytical Chemistry, 613, 131–138, 2008, DOI: doi.org/10.1016/j.jelechem.2007.10.017.
[25] Maxwell Technologies Enabling Energy's Future, 2.7V 650-3000F Ultracapacitor cells, BCAP series datasheet, 2019.
[26] W. Cantor, E. Davis, D. Feder, M. Hlavac, Performance measurement and reliability of VRLA batteries - Part II: the second generation, Advanced Data Services, Chicago, IL, USA, DOI: 10.1109/INTLEC.1998.793528.
[27] S. Elia, A. Ruvio, D. Bracci, A study on a high-reliability electromechanical undervoltage relay immersed in natural ester oil: application in mutual aid system for gensets using, IEEE 20th International Conference on Dielectric Liquids (ICDL), Rome, Italy, 2019, DOI: 10.1109/ICDL.2019.8796685.
[28] IEEE, STD 493-2007 Recommended Practice for the Design of Reliable Industrial and Commercial Power Systems, 2007.
[29] Perkins, Technical Data 4000 series, Diesel Engine-Electrounit, 4008TAG-4008TAG1-4008TAG2 datasheet, 2001.
[30] H. Yang, Analysis of Supercapacitor Charge Redistribution through Constant Power Experiments, IEEE Power & Energy Society General Meeting, Chicago, IL, USA, 2017, DOI: 10.1109/PESGM.2017.8274520.
[31] T.D. Iveland, Selection criteria for diesel cranking batteries, Third Int. Telecommunications Energy Conf., London, England, 1981.
[32] C. Boccaletti, M. Macilletti, Electrical Storage Systems in Cogeneration Plants Based on the Solar Energy Source, Int. Conf. on Clean Electrical Power, Ischia, Italy, ISBN: 978-1-4244-8929-9, DOI: 10.1109/ICCEP.2011.6036374, 2011.
[33] Hammond Manufacturing, Heavy Current Chassis Mount, 195-196 series datasheet, 2018.
[34] M. Kermani, G. Parise, L. Martirano, L. Parise, B. Chavdarian, Utilization of Regenerative Energy by Ultracapacitor Sizing for Peak Shaving in STS Crane, 2019 IEEE Int. Conf. on Environment and Electrical Engineering and 2019 IEEE Industrial and Commercial Power Systems Europe, 2019, 8783770, DOI: 10.1109/EEEIC.2019.8783770.